

# 行政院國家科學委員會專題研究計畫期末報告

## 在均勻強勢對流中紊流場及不同溫度對液滴蒸發及引燃行為影響之研究

### Effects of Free-Stream Turbulence and Temperature on the Evaporation and Ignition of A Single Liquid Droplet (3/3)

計畫編號：NSC 90-2212-E-009-085

執行期限：89年8月1日至90年7月31日

主持人：吳宗信 國立交通大學機械工程學系

#### 中文摘要

本文章主要報告本計畫執行結果。本研究主要採用實驗的方式進行一系列燃油液滴蒸發之探討，首先嘗試找出可人為控制的紊流流場，並且研究燃油液滴蒸發與紊流場中紊流強度的相互關係，然後再深入瞭解紊流場中各種特徵長度尺度與燃油液滴蒸發間影響的因素。在實驗方法上，乃是採用雷射都卜勒測速儀(LDA)來量測流場的基本性質，找出紊流場中具均質性(homogeneous)與等向性(isotropic)的區域範圍，以決定液滴實驗中液滴的測試位置。液滴蒸發方面，則是藉由高解析度的數位攝影機及影像擷取卡之助，利用背光法的拍攝技巧，在不同性質流場下進行液滴蒸發的拍攝，以供往後液滴蒸發之分析。

本文主要討論可分為兩大部分，第一部份先探討中低速風洞的特性，其中包括常溫典型圓管紊流場的平均速度分佈剖面、速度擾動分佈剖面及常溫高紊流場的平均速度分佈剖面、速度擾動分佈剖面，並觀察測試段從上游至下游的平均速度與速度擾動的變化情形。另外也對不同紊流強度的多種常溫流場之速度分佈剖面、速度擾動剖面、測試段上下游間的變化、能量頻譜、速度擾動之概率密度函數分析(PDF, Probability Density Function)等，做完整全面性的探討。

本研究中所使用的數種不同燃料液滴包括正戊烷(Pentane,  $C_5H_{12}$ )、正己烷(Hexane,  $C_6H_{14}$ )、正庚烷(Heptane,  $C_7H_{16}$ )、正辛烷(Octane,  $C_8H_{18}$ )、正癸烷(Decane,  $C_{10}H_{22}$ )，本文在第二部份則是探討利用不同的燃料液滴在不同紊流強度及尺度流場下液滴蒸發之情形，除了討論 vaporization Damkohler number 對液滴蒸發的影響外，也比較 Gokalp et al. (1992)的實驗結果與本文實驗結果之異同，並更深入探討流場中的各種特徵長度尺度對液滴蒸發的影響，嘗試找出紊流場中流場性質及燃油液滴本身特性，來決定影響液滴蒸發重要之參數，並找出其相互之關係，以期許對相關液滴蒸發的研究及應用

**關鍵詞：**液滴蒸發、紊流強度、紊流大尺度(Integral length scale)

#### Abstract

This report mainly describes the final report of

the current NSC project in two folds: (1) the experimental results of the droplet (hexane, heptane, octane and decane) evaporation at various turbulence integral length scale and turbulence intensities in ambient temperature.

**Keywords:** free-stream turbulence, integral length scales, droplet evaporation.

#### I. Introduction

Because of the importance of fundamentals and applications to spray combustion, liquid droplet evaporation has been studied intensively in the past, for details see Faeth [1] and Sirignano [2]. In the practical spray system, the liquid droplet evaporation phenomena is very complicated, comprising the liquid phase, the fuel vapor phase and the surrounding forced convection with turbulence, and the interactions among each others. Not only the understanding of liquid droplet evaporation is crucial in essence, it also plays an important role in determining the ignition time delay and ignition location of droplets.

There are numerous research conducted in the past attempting to study the evaporation process in a single liquid droplet [3]. Most experimental studies were carried out for a single liquid droplet in natural convection or laminar forced convection, while very few has been made to study the effects of turbulence in forced convection. On the other hand, most numerical studies has assumed no free-stream turbulence effects on the droplet evaporation rates, since the size of large eddy in the free stream turbulence is much larger than the droplet diameter, indicating the local laminar flow exists from viewpoints of droplet [4]. However, free-stream turbulence is composed of continuous spectrum of various length scales and time scales. Hence, there exists other smaller length and time scales in the turbulence that might effect the evaporation rate of liquid droplets.

Based on these observations, the present experimental investigation was undertaken to better understand the evaporation of a single liquid droplet in turbulent environments. The study involved detailed laser velocimetry measurement of ambient mean velocities and turbulence properties at the exit of a

nozzle-like wind tunnel, and the vaporization rates of a single liquid droplet in turbulence environments using high-speed CCD camera. For the droplet evaporation in ambient temperature, test conditions are summarized as follows:  $Re=100$ , ambient turbulence intensities from 1.0% to 60%,  $d$  of 2.5-20. These conditions represent the excellent tests to the assumption of local laminar flow conditions imposed in the past research on evaporation of the single liquid droplet. While for the progress of the construction of a high-temperature, turbulent wind tunnel is reported in the section of experimental methods.

## II. EXPERIMENTAL METHODS

### Droplet Evaporation in Ambient Temperature

A sketch of the experimental apparatus is illustrated in Fig. 1, which has been modified to produce wider ranges of the turbulence scales and integral lengths. Detailed description about the apparatus has been described in the midterm report and will be skipped here. A disk with diameters of 60 mm and 20 mm is placed in the up flowing turbulent pipe to produce the required turbulence properties, as illustrated in Fig. 2. Changing the distance of the disk to the exit of the pipe controls the turbulence scales and turbulence intensities at the exit of the pipe. Mean and turbulent flow properties in the test section were measured using a traversible laser velocimeter with a dual-beam forward-scatter configuration, combining a 2.25:1 beam expander to yield a measuring volume of  $50\mu\text{m}$  in diameter and  $300\mu\text{m}$  in length. LDA signal processor (TSI, model IFA-750) then processes the measuring data and outputs the processed data onto a personal computer.

The fuel types of test liquid droplets include hexane, heptane, octane and decane with diameters in the range of 1.6-2.5 mm. The liquid droplet is suspended at the tip of quartz fiber with diameter of about  $100\mu\text{m}$  and placed at the location of 5 mm away from the exit of the wind tunnel. A wind-shielding plate made of stainless steel plate was placed below the test liquid droplet to prevent pre-heating/evaporation of the droplet before experiment starts. As the test liquid droplet has been injected from the syringe and moved to the top of the heat-shielding plate, the plate is moved away and a high-speed CCD camera (Kodak Motion Corder Analyzer, monochrome Model SR-Ultra) is triggered to record the image of tested liquid droplet.

### Droplet Evaporation and Ignition in High Temperature Environments

A wind tunnel, as schematically shown in Fig. 3, similar to the previous one used for low-temperature droplet evaporation. Instead a high-volume (maximum 500 l/s) air compressor drives this high-temperature

wind tunnel. A special-made electric heater (maximum exit temperature 1100K), equipped with over-temperature protection, heats up the airflow from the compressor. In addition to the installation of the insulation materials covering the wind tunnel, a wrap-around PID-controlled, electric pre-heater (can be heated up to 1100K) is installed between the bulk of the wind tunnel and the insulation to prevent the heat loss of the airflow to the body of the wind tunnel, which is made of stainless steel material. Seeding particles for laser velocimetry measurements are supplied by a manifold from the main airflow before the inlet to the high-temperature air heater. At this moment, the construction is completed and the preliminary tests show that the airflow can be heated up to 1050K at the exit of the wind tunnel, with the help of the pre-heater, without the contraction. Hopefully, this will provide an easy way, as compared with the post-flame type wind tunnel, to produce the required turbulence properties. Indeed, the air temperatures obtained using the blow-type wind tunnel is lower than that using post-flame region of a flat-flame; however, this setup represents an excellent test facility, which provides a high-temperature turbulent environment for droplet evaporation and ignition research.

## III. RESULTS AND DISCUSSION

In this section, results are presented for the results of the droplet evaporation without ambient turbulence (quasi-laminar) and with the variations of turbulence scales and turbulence intensities are described next. In addition, only results at room temperature are described in the following.

### **Evaluation of the Apparatus**

The evaluation of the apparatus is mainly focused on the uniformity of mean and fluctuating velocity distributions and the temporal power spectra in the regions of interest and has been described in detail in the midterm report.

### **Summary of Test Conditions**

In summary, the resulting turbulence intensities and integral length scales are in the range of 1-30 mm and 1-55%, respectively. Reynolds number are in the range of 72-333, based on the mean speed of the airflow and the diameter of the suspended droplet, to have wider ranges of turbulence intensities and scales using the current test facility. The resulting mean speed ranges in 0.6-1.0 m/s, depending upon the droplet size (1.6-2.5mm). Detailed test conditions are skipped due to the constraint of the length of the report.

### **Droplet Evaporation in quasi-laminar environments**

Typical results of normalized droplet evaporation rate, with respect to natural evaporation rate, as a function of  $Re^{1/2} Sc^{1/3}$ , for hexane, heptane, octane and decane, in quasi-laminar environments are

illustrated in Fig. 4. All data are correlated reasonably well and the slope (0.27) is consistent with the results of Frossling et al (1938) within experimental uncertainties. As can be seen, evaporation rate increases with  $Re^{1/2} Sc^{1/3}$

### Droplet Evaporation in turbulent environments

Fig. 5 illustrates the normalized evaporation rate ( $K/K_L$ ) as a function of  $Da_v$  (effective evaporation Damkohler number) for all the test fuels (hexane, heptane, octane and decane) and Reynolds number (72-333), which illuminates the influence of ambient turbulence. There are two distinct regimes considering the variations of  $K/K_L$  with respect to  $Da_v$ . For  $Da_v < 0.1$ , normalized evaporation rate correlated as  $K/K_L = 0.771 Da_v^{-0.111}$ , which represents strong ambient turbulence effects. For  $Da_v > 0.1$ , however, normalized evaporation rates are approximately constant, which represents weak ambient turbulence effects.

### REFERENCE

1. Faeth, G.M., *Prog. Energy Com. Sci.*, Vol.9, pp.1, 1983.
2. Sirignano, W.A., *Prog. Energy Com. Sci.*, Vol.9, pp.291, 1983
3. Frossling, N. *Gerlands Beitrage zur Geophysik*, Vol.52 (1/2), p.170, 1938.
4. Megaridis, C.M. and Siriginano, W.A., *ASME Winter Meeting*, Dallas, Texas, 1990.

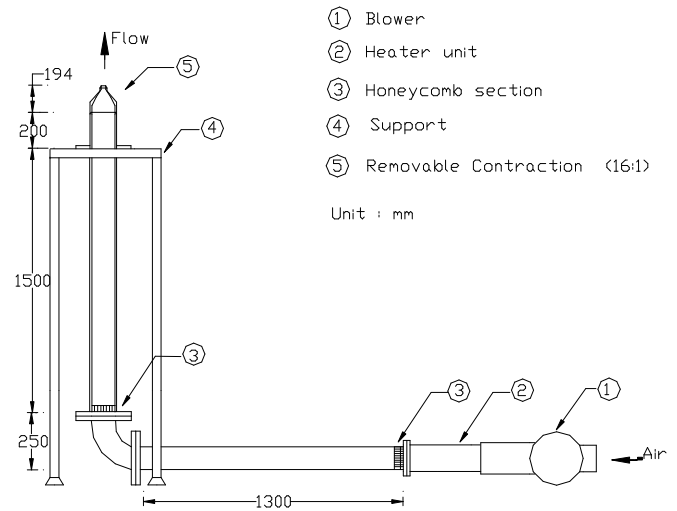


Figure 2.1 Schematic diagram of wind tunnel.

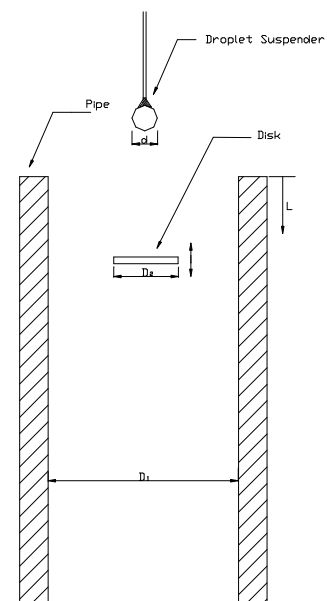


Figure 2.2 Schematic diagram of turbulence generator

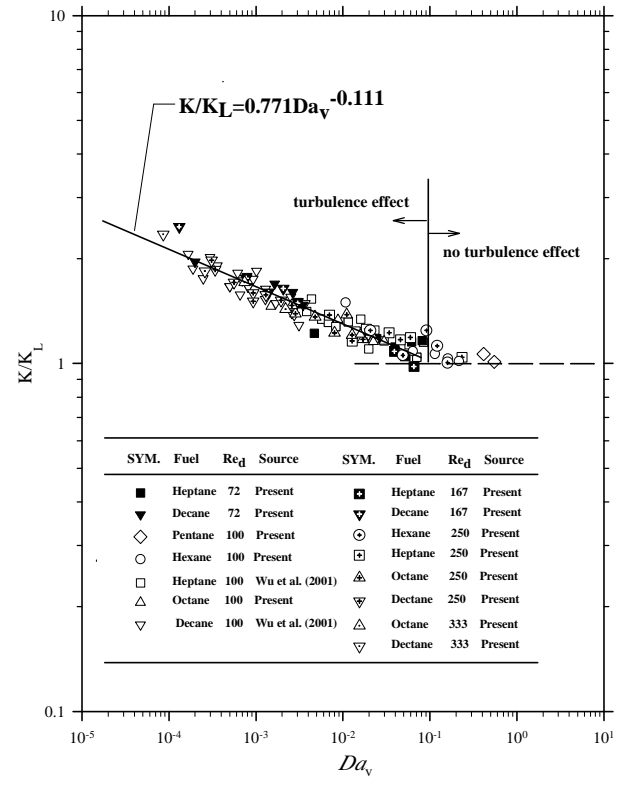
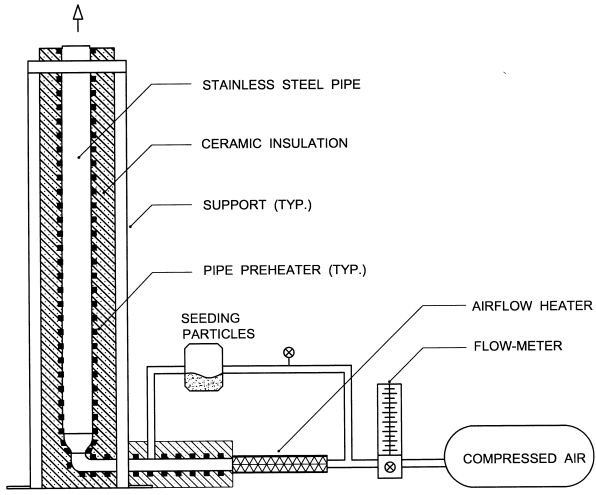


Figure 5.15 Variations rate of vaporization rate compared with laminar vaporization rate to Damkohler number for different fuels

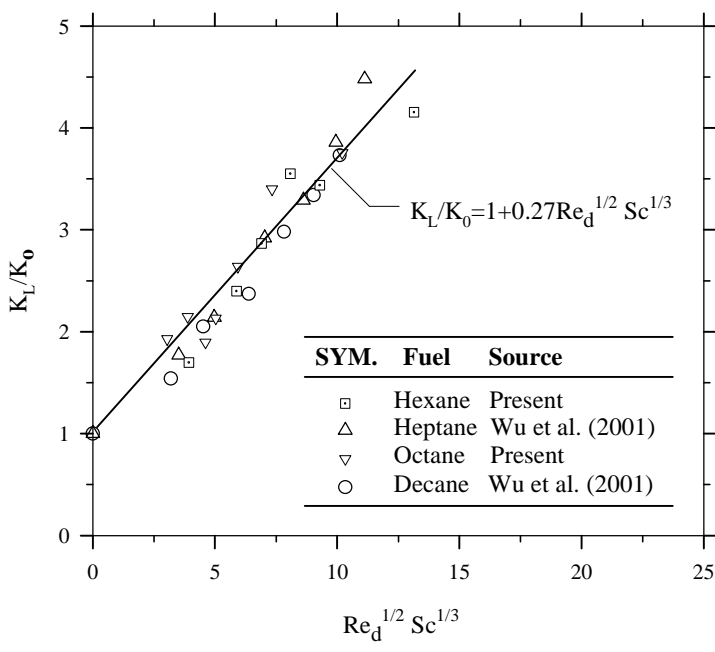


Figure 5.3 Check for Frossling correlation for different fuels